10th World Congress on Structural and Multidisciplinary Optimization
May 19 -24, 2013, Orlando, Florida, USA

Designing flapping wings as oscillating structures

Zhiyuan Zhang[1], Ashok V. Kumar[2], Raphael T. Haftka[3]

[1] University of Florida, Gainesville, Florida, USA, z.zhang@ufl.edu
[2] University of Florida, Gainesville, Florida, USA, akumar@ufl.edu
[3] University of Florida, Gainesville, Florida, USA, haftka@ufl.edu

1. Abstract

Micro air vehicles propelled by flapping wings are gaining interest for certain applications because flapping can provide more agility and maneuverability at low speeds. Flapping wings must deform in certain shapes to produce maximum lift and thrust. In this paper, we show that one can tailor the flapping wing's forced response to approximate a desired response. When the desired flapping motion is a harmonic oscillation, the desired response can be described by the shape of the steady state response. For non-harmonic flapping of the wing, the desired response is defined by motion at points along the wing as a function of time. Data is available in references for the motion of the tip and wrist of the humming bird wing as it flaps. The motion at the tip and wrist of the wing at flying speed equals to 12m/s is used as the desired motion. Fourier transform of this motion reveals the frequencies of interest. The base excitation is assumed to be a combination of flapping motion and forward-backward motion. These input base motions are functions of time and must be optimized to obtain the desired response. To parameterize these input motions, it is convenient to express them as a truncated Fourier series. The amplitudes in the Fourier series are then the design variables / parameters to be optimized. The structural dynamics of the wing is optimized to match the desired motion using ply orientation as a design variable to minimize the difference between the desired and the computed response. The forced response of the wing is computed using finite element analysis.

2. Keywords: Flapping Wing, Structural Optimization, Dynamic Analysis

3. Introduction

Micro air vehicles (MAVs) are widely used in environmental monitoring, surveillance and military. Different MAVs concepts have been developed, such as fixed wing, rotary wing, flapping wing etc. MAVs operate in low Reynolds number regime, and a common feature of the birds and insects is that they have flapping wings. This may indicate that flapping is advantageous in low Reynolds number flight. Some birds, bats and insects have similar dimensions and flight speed as MAVs, which can provide us with intuition on how to design a prototype. Compared with fixed wing MAVs, flapping wing MAVs can be more maneuverable. Flapping wings must deform in certain shapes to produce maximum lift and thrust. Tailoring the flapping wing's forced response to match a desired response is the subject of this paper.

Wu, Ifju and Stanford [1] analyzed the relationship between the aerodynamic forces for hovering flight and wing structure and concluded that wing stiffness is crucial in thrust production: only certain modes of passive aeroelastic deformation allow the wing to effectively produce thrust. Tuncer and Kaya [2] maximized the thrust and/or propulsive efficiency of an airfoil flapping. They found that high thrust values may be obtained at the expense of propulsive efficiency and the effective angle of attack has to be reduced which ultimately prevents the formation of leading edge vortices for a high propulsive efficiency.

Stanford, Beran and Kobayashi [3] used cellular division method coupled with genetic algorithm for obtaining optimal wing structural topologies, and provided an understanding of the key relationships between skeletal topology, aeroelastic behavior, and performance metrics during flapping flight. Stanford, Kurdi, Beran, and McClung [4] have used wing shape, wing structure, and kinematic motions as the design variables to minimize the peak power input to a flexible hovering wing. Their aeroelastic model coupled a three-dimensional nonlinear beam model to a quasi-steady blade element aerodynamic model.

Using CFD computation to calculate the performance of the flapping wing is computationally expensive, so it is helpful if we convert the optimization problem to mimic a desired motion, which can generate maximum thrust and lift. The desired shape can be obtained from high-speed photographs of birds or insects. The objective of the present note is to demonstrate that achieving a desired flapping motion of hummingbird wing with reasonable accuracy is possible using a Fourier expansion expression for the input or excitation force / displacement.

4. Desired Motion

When the desired flapping motion is a harmonic oscillation, the desired response can be described by the shape of the steady state response. For non-harmonic forced response we need displacements, at a few locations on the wing, as a function of time. In both cases, we want to optimize the structural parameters and input base excitation to minimize the error in forced response from the desired response. High speed video of hummingbird wings is used as reference to specify desired response. Tobalske et al [5] studied the kinematics of hummingbird flight and used synchronized high-speed video cameras to measure the three-dimensional wing kinematics. We treat this hummingbird's motion as the desired motion. The motion at points along the wing obtained from reference [5] was used for this study. We assume that the wings are made of graphite/epoxy laminated composite and shaped like humming bird wings with a maximal dimension of 15 cm and flight speeds up to 12m/s. When the wing is flapping in a harmonic motion, it can be designed to oscillate in a desired fashion using both the base excitation parameters and structural parameters. Base excitation parameters can be the amplitude of flapping, heaving and pitching motions as well as frequency. Several structural parameters could be optimized including ply orientations, number of layers, distribution of point masses and the shape of the wing and its attached stiffeners. In this work we only use ply orientation for the optimization.

In order to simplify the problem, two points, tip and wrist, are compared instead of all the points on the wing. For forward flying (12m/s), the beat frequency is 42Hz and the stroke-plane angle relative to horizontal is 67.26 °. Figure 1 shows the tip and wrist motion path of the wing (from [5]). For the coordinate system, x-direction is horizontal, z-direction is vertical and y-direction is perpendicular to x and z direction. Another coordinate system is created to simplify the process of modeling and simulation and is shown in Fig. 1 as the blue coordinate system. In this coordinate system, x' direction is perpendicular to stroke plane of the wing, y' direction is the same as y direction and z' direction is perpendicular to the plane defined by the x' and y'.

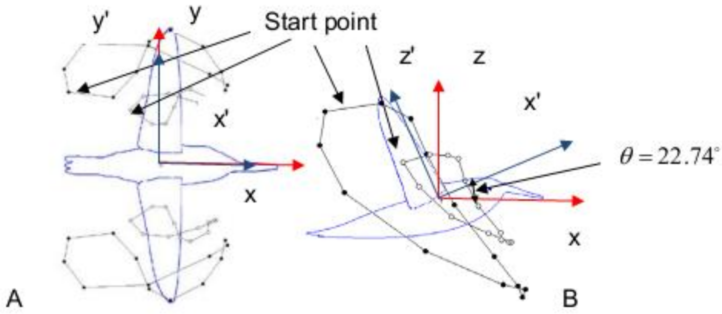

Figure 1: Coordinate systems for humming bird A) dorsal view, B) lateral view (based on [5])

The motion of the wing can be decomposed into three parts: flapping motion, pitching motion and forward-backward motion. Only the flapping motion and forward-backward motion are considered here because motion at only two points on the wing is available. Figure 2 and 3 show Fast Fourier Transformation (FFT) of the motion of wingtip and wrist. The x'-direction motion (forward-backward) can be regarded as rigid body motion due to the high stiffness in that direction. Therefore, the following analyzes is focused on the flapping motion and only the z' displacement is considered. From Fig. 1 and Fig. 2 we see that the amplitudes at 42Hz, 84Hz and 126 Hz are the dominant frequencies.

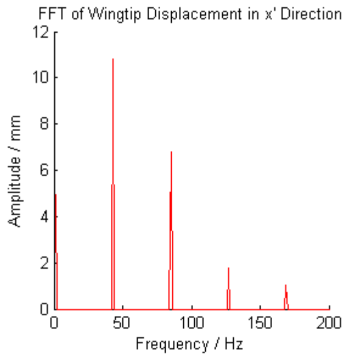

(A)

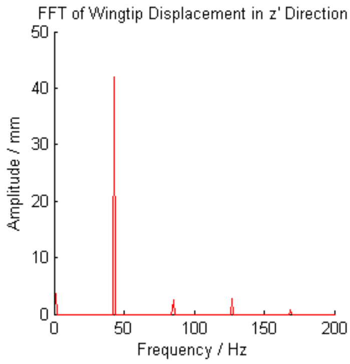

(B)

Figure 2: FFT of wing tip displacement A) x' direction (forward-backward) B) z' direction (flapping)

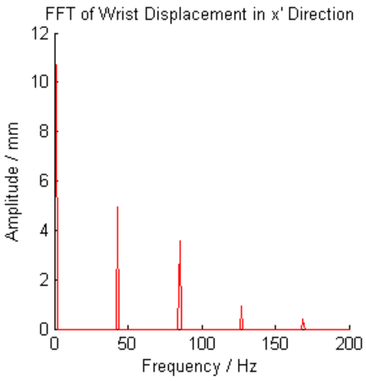

(A)

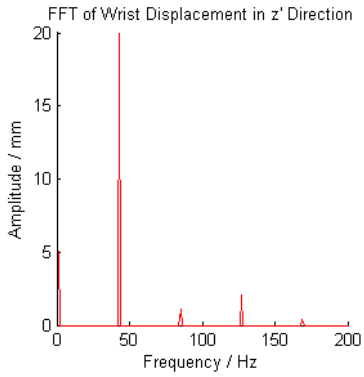

(B)

Figure 3: FFT of wrist displacement A) x' direction B) z' direction

5. Optimal structure and input excitation

The geometry of the wing used for the analysis is shown in Fig. 4. It is flapped by input excitation at the base near the coordinate system and this input motion as well as the wing must be designed to mimic the wing movement of the hummingbird. The length of the wing = 47 mm, the average wing chord = 12 mm, the single wing area = 558mm^2 and the total thickness = 0.25 mm.

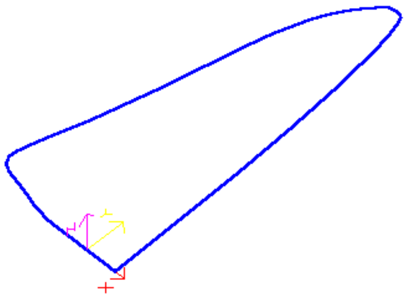

Figure 4: Flapping wing shape (based on [5]) for dynamics response based design

The flapping motion is assumed to be induced by rotational base excitation which we can express as a Fourier series using frequencies that are dominant in the desired output motion. The base excitation is therefore expressed as the following angular displacement as a function of time:

$$\begin{aligned}\theta(t) &= \alpha_0 + \alpha_1 \sin(\frac{42}{2\pi}t) + \beta_1 \cos(\frac{42}{2\pi}t) \\ &+ \alpha_2 \sin(\frac{42}{\pi}t) + \beta_2 \cos(\frac{42}{\pi}t) + \alpha_3 \sin(3\frac{42}{2\pi}t) + \beta_3 \cos(3\frac{42}{2\pi}t)\end{aligned} \tag{1}$$

The output response can be expressed as a superposition of the steady state response of each term in the input excitation. If the frequency response due to unit input at the wing tip are A_i, $i = 0,1,2,3$, for the frequencies 0, 42, 84 and 126Hz respectively and B_i, $i = 0,1,2,3$ are the response for these frequencies at the wing wrist, then we can write the response at the tip and wrist as follows

$$\begin{aligned}w_{actual}^{tip}(t) &= A_0\alpha_0 + A_1\alpha_1 \sin(\frac{42}{2\pi}t) + A_1\beta_1 \cos(\frac{42}{2\pi}t) \\ &+ A_2\alpha_2 \sin(\frac{42}{\pi}t) + A_2\beta_2 \cos(\frac{42}{\pi}t) + A_3\alpha_3 \sin(3\frac{42}{2\pi}t) + A_3\beta_3 \cos(3\frac{42}{2\pi}t)\end{aligned} \tag{2}$$

$$\begin{aligned}w_{actual}^{wrist}(t) &= B_0\alpha_0 + B_1\alpha_1 \sin(\frac{42}{2\pi}t) + B_1\beta_1 \cos(\frac{42}{2\pi}t) \\ &+ B_2\alpha_2 \sin(\frac{42}{\pi}t) + B_2\beta_2 \cos(\frac{42}{\pi}t) + B_3\alpha_3 \sin(3\frac{42}{2\pi}t) + B_3\beta_3 \cos(3\frac{42}{2\pi}t)\end{aligned} \tag{3}$$

We denote the desired motion in z' direction at the tip as $w_{desired}^{tip}(t)$ and at the wrist as $w_{desired}^{wrist}(t)$. The differences between actual and desired motion at the data points available represent the error during the whole period of flapping. Then, we can write the objective function as:

$$\text{Minimize: } \Pi = r^{tip}\left\|\mathbf{w}_{actual}^{tip} - \mathbf{w}_{desired}^{tip}\right\|^2 + r^{wrist}\left\|\mathbf{w}_{actual}^{wrist} - \mathbf{w}_{desired}^{wrist}\right\|^2 \tag{4}$$

Where,

r^{tip} and r^{wrist} are the weighting factors for the tip and wrist errors
$\mathbf{w}_{actual}^{tip}$ = Actual displacement vector in z' direction of wing tip
$\mathbf{w}_{desired}^{tip}$ = Desired displacement vector in z' direction of wing tip
$\mathbf{w}_{actual}^{wrist}$ = Actual displacement vector in z' direction of wrist
$\mathbf{w}_{desired}^{wrist}$ = Desired displacement vector in z' direction of wrist

In order to find the optimal value of coefficients α_0, α_1, α_2, α_3, β_1, β_2 and β_3, we set the derivative of objective function with respect to α_0, α_1, α_2, α_3, β_1, β_2 and β_3 to zero and solve the resulting equation to get the optimal values of these coefficients to determine the optimal input $\theta(t)$.

Two steps will be used here for designing the wing. In the first step, we assume that the wing is made of a very stiff material, so that the motion of the wing could be regarded as rigid body motion. The optimal input, expressed as a truncated Fourier series, is determined to produce an output dynamic response which mimics best the measured motion of the hummingbird wing. In the second step, we assume that the wing is made of four-ply symmetric and balanced graphite/epoxy laminate. The material stiffness will vary with the ply angle. The optimal angle is selected to minimize the different between the dynamic response and measured motion of hummingbird wing.

6. Results and discussion

6.1 Stiff Wing Design

In this step we assume the material of wing is very stiff and that the wing motion behaves like a rigid body motion. The material was assumed to be isotropic with E=2.0e12Pa. The eight constants A_0, A_1, A_2, A_3, B_0, B_1, B_2 and B_3 are computed based on frequency response computed using finite element analysis. We can minimize just the error at the tip by setting r^{tip} =1 and r^{wrist} =0, or we can minimize the error at the wrist alone by setting r^{tip} =0 and r^{wrist} =1. To minimize both errors simultaneously we have set the weighting factors r^{tip} =0.25 and r^{wrist} =1. As we are using a linear finite element model, which cannot accurately predict large motions, the desired tip and wrist displacement are reduced to one third of the real measured result.

Figure 5 shows the actual optimal displacement in z' direction at wing tip and wrist when we only minimize the error at the tip. The displacement at wing tip matches perfectly the desired motion, but they do not match well at the wrist. Figure 6 shows the result when we only minimize the error at the wrist. The actual and desired motions match well at the wrist, but not match at the tip. Figure 7 shows displacement result in z' direction at wing tip and wrist when we minimize the error from both wing tip and wrist. It indicates that minimizing the error at both the wing tip and wrist is necessary to get the best results.

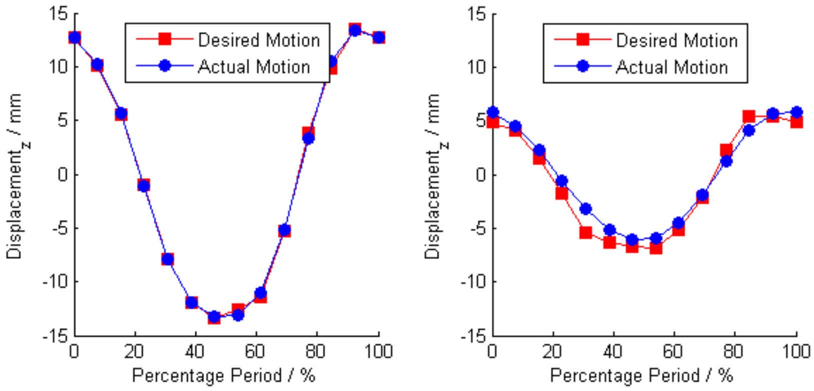

Figure 5: The optimal result when only minimize the error at the wingtip A) Displacement at wingtip, B) Displacement at wrist for a rigid wing

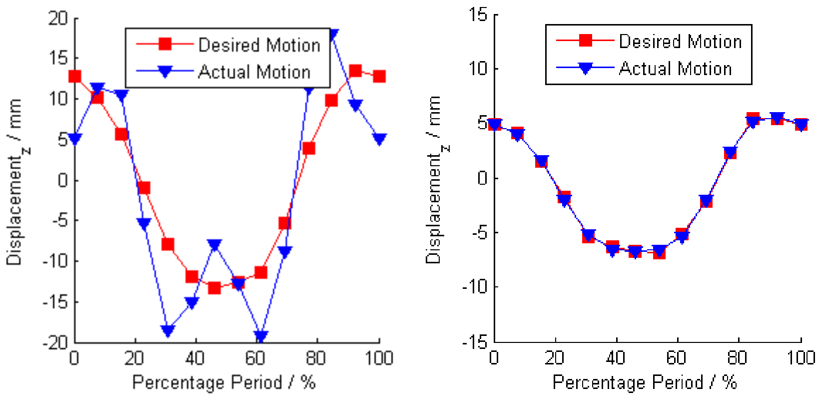

Figure 6: The optimal result when only minimize the error at the wrist A) Displacement at wingtip, B) Displacement at wrist for a rigid wing

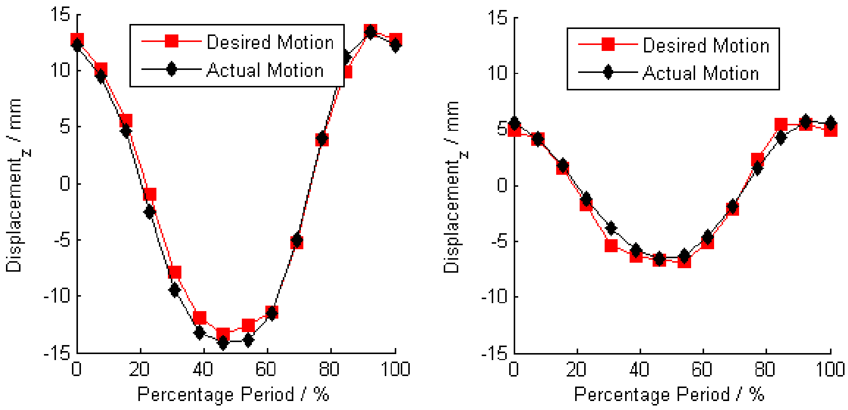

Figure 7: The optimal result when only minimize the error at the wingtip and wrist A) Displacement at wingtip, B) Displacement at wrist for a rigid wing

6.2 Composite Wing Design

Inspired by the result of high stiffness wing that there are some dynamic deformation of the flapping wing, we seek the optimal composite wing whose response at the tip and wrist best matches the measured response. The same wing geometry is used here as in stiff wing design. A $[+\theta/-\theta]_S$ graphite/epoxy laminate composite material is used. Each ply is transversely isotropic with elastic constants defined as: $E_1 = 1.81\times10^{11}$ Pa, $E_2 = 1.03\times10^{10}$ Pa, $\nu_{12} = 0.28$, $G_{12} = G_{13} = 7.17\times10^9$ Pa, $G_{23} = 5.07\times10^9$ Pa and density $\rho = 1550$ kg/m^3. The ply angle is optimized to minimize the error defined in Equation (5), which is a root mean square (RMS) error normalized by the absolute maximum displacement in a period. Figure 8 shows the normalized error values for ply angle. It indicates that when considering errors from both wingtip and wrist to optimize the input, we can get the smallest error. The optimal ply angle is 70 degrees when we minimize the error from wingtip and wrist.

$$\text{Normalized Error} = \sqrt{\frac{\left\|\dfrac{\mathbf{w}_{actual}^{tip} - \mathbf{w}_{desired}^{tip}}{\text{Max}(\mathbf{w}_{desired}^{tip})}\right\|^2 + \left\|\dfrac{\mathbf{w}_{actual}^{wrist} - \mathbf{w}_{desired}^{wrist}}{\text{Max}(\mathbf{w}_{desired}^{wrist})}\right\|^2}{\text{Number}(\mathbf{w}_{desired}^{tip}) + \text{Number}(\mathbf{w}_{desired}^{wrist})}} \tag{5}$$

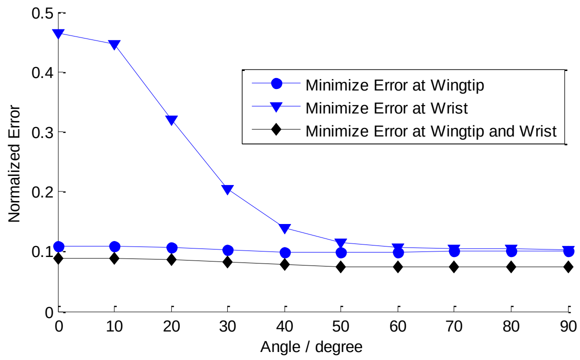

Figure 8: The normalized error as function of ply angle.

Figure 9 shows the actual optimal displacement in z' direction at wing tip and wrist when we only minimize the error at the tip and the ply angle is 50 degrees. Figure 10 shows the result when we only minimize the error from wrist and the ply angle is 90 degrees. Figure 11 shows displacement result in z' direction at wing tip and wrist when we minimize the error from both wing tip and wrist at ply angle of 70 degrees. We can find that when we only minimize the error from tip, the motion will not match at the wrist. When we can make the wrist motion matches, the difference at the wing tip get large. So we need to sacrifice the accuracy both at the wing tip and wrist and get compromised result as in figure 11.

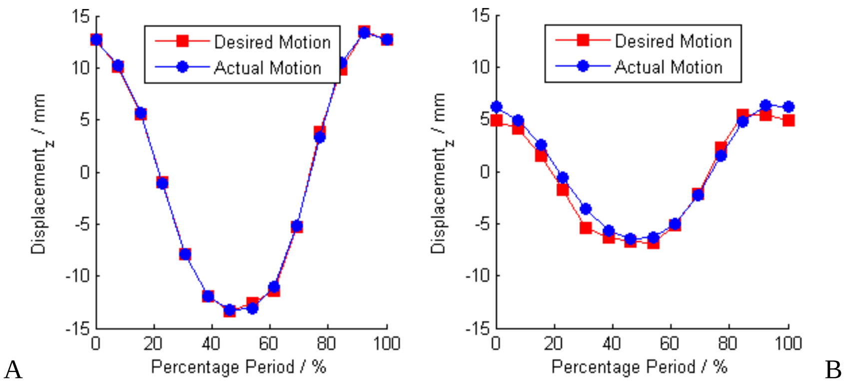

Figure 9: The optimal result when we only minimize the error at the wingtip A) Displacement at wingtip, B) Displacement at wrist

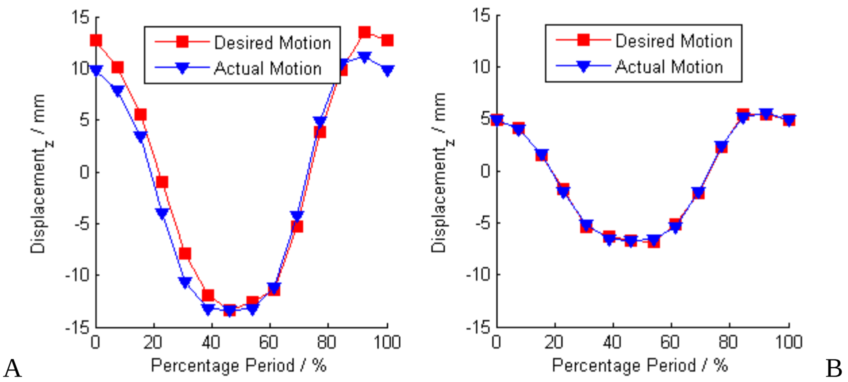

Figure 10: The optimal result when we only minimize the error at the wrist A) Displacement at wingtip, B) Displacement at wrist

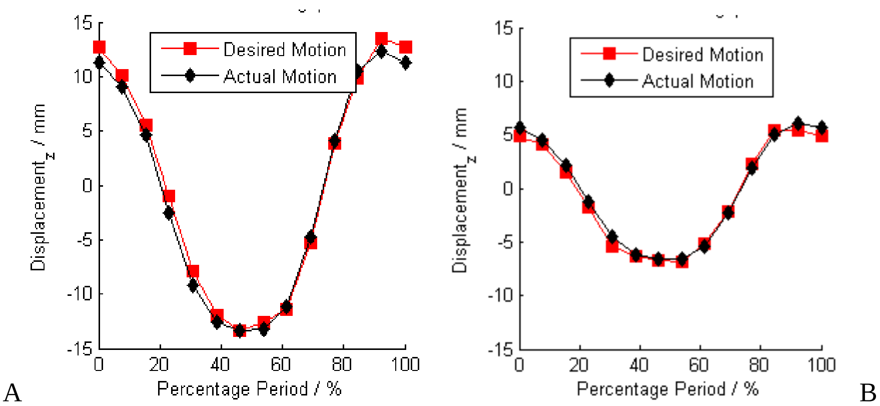

Figure 11: The optimal result when only minimize the error at the wingtip and wrist A) Displacement at wingtip, B) Displacement at wrist

6. Conclusion

This paper has presented a method for controlling the dynamic response of a flapping wing. It is shown that the flapping displacement at wingtip and wrist can be approximated well. We assumed that the input base excitation was a Fourier series. The results show that we can approximate the desired flapping motion of the wing to a reasonable level of accuracy by optimizing the ply orientation and the Fourier expansion amplitude of base excitation flapping angle. The other two motion pitching and forward and backward motion are mostly rigid body motion. So, these two motions can be achieved easily by applying a relevant input. It will be interesting to conduct further studies by including aerodynamic forces to get a more reality structural optimization result.

7. References

[1] P. Wu, P. Ifju and B. Stanford, Flapping Wing Structural Deformation and Thrust Correlation Study with Flexible Membrane Wings, *AIAA Journal*, 48 (9), 2111-2122, 2010.

[2] I.H. Tuncer and M. Kaya, Optimization of flapping airfoils for maximum thrust and propulsive efficiency, *AIAA Journal*, 43 (11), 2329-2336, 2005.

[3] B. Stanford, P. Beran and M. Kobayashi, Aeroelastic optimization of olapping wing venation: a cellular division approach. *52nd AIAA/ASME/ASCE/AHS/ASC Structures, Structural Dynamics and Materials Conference*, Denver, CO, 2011, AIAA 2011-2094.
[4] B. Stanford, M. Kurdi, P. Beran and A. McClung, Shape, Structure, and Kinematic Parameterization of a Power-Optimal Hovering Wing, *AIAA* 2010-2963.
[5] B.W. Tobalske, D.R. Warrick, C.J. Clarket, D.R. Powers, T.L. Hedrick, G.A. Hyder and A.A. Bieweneral, Three-dimensional kinematics of hummingbird flight, *The Journal of Experimental Biology*, 210 (13), 2368-2382, 2007.